Journal of Applied Polymer Science

Solution blown sulfonated poly(ether sulfone)/poly(ether sulfone) nanofiber-Nafion composite membranes for proton exchange membrane fuel cells

Hang Wang,[1] Xupin Zhuang,[1,2] Xiaojie Li,[1] Wei Wang,[1] Yannan Wang,[1] Bowen Cheng[2]

[1]College of Textile, Tianjin Polytechnic University, Tianjin 300387, People's Republic of China

[2]Key Laboratory of Advanced Textile Composite Materials of Ministry of Education, Tianjin Polytechnic University, Tianjin 300387, People's Republic of China

Correspondence to: X. P. Zhuang (E-mail: zhxupin@tjpu.edu.cn)

ABSTRACT: A composite membrane of sulfonated poly(ether sulfone) (SPES)/poly(ether sulfone) (PES) nanofiber (NF) mat impregnated with Nafion was prepared and evaluated for its potential use as a proton conductor for proton exchange membrane (PEM) fuel cells. The supporting composite nanofibrous mat was prepared by solution blowing of a mixture of SPES/PES solution. The characteristics of the SPES/PES NF and the composite membrane, such as morphology, thermal stability, and performance of membrane as PEMs, were investigated. The performance of composite membranes was compared with that of Nafion117. The introduction of solution blown NFs to composite membranes modestly improved proton conductivity, water swelling, and methanol permeability. Therefore, composite membrane containing SPES/PES NFs can be considered as a novel PEM for fuel cell applications. © 2015 Wiley Periodicals, Inc. J. Appl. Polym. Sci. **2015**, *132*, 42572.

KEYWORDS: fibers; membranes; nanostructured polymers; properties and characterization

Received 1 April 2015; accepted 1 June 2015
DOI: 10.1002/app.42572

INTRODUCTION

Fuel cells can convert the chemical energy of a fuel into electricity, and are widely considered to be promising green, reliable, and efficient power sources that offer higher energy densities and energy efficiencies compared to other current systems.[1,2] Among several types of fuel cells, proton exchange membrane fuel cells (PEMFCs) have received considerable attention. Development and research on PEMFC have been an active area in recent years. The most important part of PEMFCs is their polymer electrolyte membrane, which is also known as proton exchange membranes (PEMs).[3]

Perfluorinated sulfonic acid membranes, such as Nafion, are widely used; Nafion has good thermal and chemical stability, long-term durability, and high proton conductivity at low operating temperatures. However, Nafion has numerous drawbacks that limit its applications in PEMFCs, especially in direct methanol fuel cells (DMFCs); the drawbacks include high cost, high permeation rate of methanol, poor proton conductivity at a high temperature, and poor mechanical properties under swollen conditions.[4]

Several routes have been proposed to achieve high-performance PEM with excellent proton conduction,[5] methanol crossover,[6] and mechanical properties.[7] Making composite membranes or a blend membrane with organic or inorganic matters is a common method. Recently, the nanofiber (NF) with a diameter of 200–500 nm, have drawn great attention are used as a novel filler to produce type of membranes applied to DMFC. NF usually possesses a large effective surface area and superior mechanical properties. The dimension and mechanical properties of NF composite membranes (NCMs) are greatly improved in comparison with those of conventional solvent-casting membranes. NF mats (NFMs) are usually used to be a reinforcement embedded in a polymer matrix to prepare a high-performance membrane. With much proton-conducting groups along the NF, NF could establish proton-conducting channels to increase proton conductivity. Hence, NCMs have been developed as a new method in the synthesis of novel PEM.[8]

Solution blowing process (SBP) has been reported as a promising NF spinning process,[9] and has generated significant interest.[10–15] In this process, a high-speed gas flow is used to blow polymer solution streams to NFs through a needle. Nylon 6,[13] Polyacrylonitrile,[14] poly(lactic acid), polyvinyl alcohol,[15] polyvinylpyrrolidone, and cellulose microfibers and NFs have been successfully produced by SBP,[10] and their diameters are close to those made by electrospinning. Compared with electrospinning,

SBP is easier to handle, has such advantages as high productivity, good mechanical property, and low energy consumption, and has been applied to DMFC materials.[16] Solution blowing is also suitable for almost all types of polymers, especially such polymers with extremely high melt viscosities. Solution blown NFs are commonly curled in three dimensions; a large number of crimped fibers are closely entangled to form a stable structure, which has numerous barrier layers and is difficult for methanol to crossover.

Considerable research has been conducted to develop alternative polymer electrolyte membrane materials.[17–21] These membrane materials are based on the modification of aromatic polymers, such as poly(ether ether ketone) (PEEK),[22] poly(ether sulfone) (PES),[23] polyphenylsulfone,[24] and polyimide.[25] To construct proton-conducting channels, sulfonated PES (SPES) was used in this study. PES is an engineering thermoplastic, which comprises repeated phenyl and sulfone groups, and has excellent mechanical properties and chemical inertness. However, the low proton conductivity of PES could limit its application as a fuel cell membrane. Sulfonation is a frequently used method to improve proton conductivity. Too high degree of sulfonation (DS), nonetheless, often leads to an unfavorable swelling of membranes and a dramatic loss in their mechanical properties.[26] To improve mechanical properties, we mixed PES into SPES solutions to prepare SPES/PES NFMs.

In this study, SPES/PES NFMs were prepared via SBP, and then mixed with different volumes of 5% Nafion. The water uptake (WU), proton conductivities, and methanol permeability, were varied with different contents of NFs in the composite membrane. The membranes were characterized through scanning electron microscope (SEM), atomic force microscope (AFM), and X-ray diffraction (XRD).

EXPERIMENTAL

Materials

PES was purchased from Changchun Institute of Applied Chemistry. N,N-dimethylformamide was obtained from Tianjin Kermel Chemical Reagent. Nafion 5 wt % solution was obtained from DuPont. All chemicals were in an analytical grade.

Syntheses of SPES

PES was dried in a vacuum oven at 100°C, and then10 g PES was added to 100 mL of concentrated (98%) sulfuric acid in a three-necked flask with vigorous stirring at 60°C. After a period of time, the reaction solution was added to ice-cold water with continuous agitation. The polymer precipitate was filtered and washed several times with distilled water until pH was close to 7. SPES was then dried at 60°C for 12 h in an air drying oven, and another 12 h in a vacuum drying oven. DS was determined by titration. SPES (1–2 g) was placed in 1*M* aqueous NaCl and kept for 1 day. The solution was titrated with 0.1*M* NaOH until pH = 7.

Fabrication of PES/SPES NFs

The experimental setup used to prepare nonwoven NFs has been shown in our previous work.[27] The polymer mixture solution had a concentration of polymer of 30 wt %. The polymer mixture was mixed in a ratio of PES/SPES = 1/9. The solution was then loaded into a syringe as spinneret. A syringe pump was used to squeeze out the spinning solution at a speed of 5 mL h^{-1} through a needle with an inner diameter of 0.5 mm, which was coaxially surrounded by a gas cavity. High velocity airflow was supplied to the gas cavity. The air pressure was 0.1 MPa. After the solution streams were pressed out of the syringe needle, the spinning solution was blown and attenuated into ultrafine fibers. The nonwoven NFs were collected on a collector to form a fibrous mat. To remove the residual solvent from the NFM, vacuum drying was conducted at 80°C for 10 h. The thickness of PES/SPES nonwoven substrate was measured to be 189 μm.

Preparation of NCMs

The solution blown PES/SPES mat was peeled off from the collector, sandwiched by a two plane steel plate, and treated with a hot-presser (CB-950Z5 hot-presser, China) at 110°C /0.5 MPa for 1 s. To prepare NCMs, PES/SPES nonwoven mat was immersed in a Nafion solution. The NCMs were dried at 30°C for 4 h. The membrane was then treated with a hot-presser at 110°C /0.1 MPa for 15 min. Finally, the membrane was dried at 90°C for 8 h in an oven. The weight-based compositions of NCM (NF/Nafion) were 20/80, 30/70, and 40/60. They were named in this study as NF/Nafion-20, NF/Nafion-30, and NF/Nafion-40, respectively.

Characterization of PES/SPES Composite Membranes

Structure and Morphology of NFMs and Composite Membranes. The morphologies of NFMs and NCMs were characterized using a SEM (Hitachi S-4800) and an AFM (CSPM5500). Before SEM observations, all samples were gold coated using a sputter coater. The membrane cross sections were obtained by immersing samples in liquid nitrogen. The diameter of fibers was determined from SEM micrographs using image analysis software.

XRD was performed using an XRD spectrometer (D8 Discover with GADDS, 40 kV, 40 mA) from 10 to 60 with a CuKa radiation ($\lambda = 1.541$ Å).

Thermal Behavior. The thermal degradation of PES and SPES was investigated by high-resolution thermogravimetric analysis (TGA), which was performed using TGA instruments (STA409PC).

Water Uptake and Swelling Ratio. WU, in-plane dimensional swelling (IS), and through-plane dimensional swelling (TS) of membranes were measured. Rectangular shaped membranes were dried in a vacuum oven at 90°C for 10 h. Their weight and length (or thickness) were then measured. After immersion in distilled water for 24 h at the desired temperature, the membranes were removed and wiped with an absorbent paper quickly. The weight and length (or thickness) were rapidly measured. WU and dimensional swelling were calculated using the following equations:

$$\mathrm{WU} = (W_w - W_d)/W_d \times 100\%$$

$$\mathrm{IS} = (S_w - S_d)/S_d \times 100\%$$

$$\mathrm{TS} = (T_w - T_d)/T_d \times 100\%$$

where W_w and W_d are the water swollen membrane weight and the dry membrane weight, respectively. S_w and S_d are the water

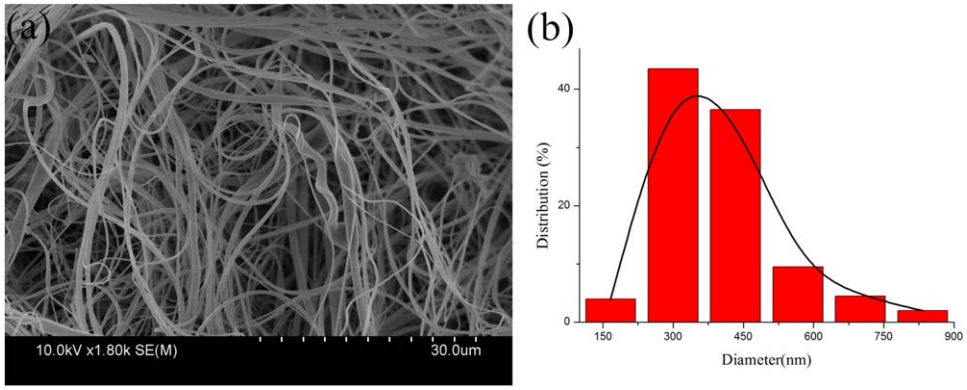

Figure 1. SEM images of SPES/PES NF and the corresponding diameter distribution map. [Color figure can be viewed in the online issue, which is available at wileyonlinelibrary.com.]

swollen membrane square and the dry membrane square, respectively. T_w and T_d are the water swollen membrane thickness and the dry membrane thickness, respectively

Proton Conductivity. The proton conductivity of samples was measured using four electrodes. The proton conductivity was measured by electrochemical impedance spectroscopy using an electrochemical workstation (CHI660D). The proton conductivity was calculated from the $\sigma = L\ A^{-1}\ R^{-1}$ formula, where L, A, and R are the membrane thickness, the cross-sectional area, and the resistance of the membrane, respectively.

Methanol Permeability. The methanol diffusion coefficient through the membrane was measured using diffusing equipment with two glass compartments, which were separated by the test membrane. A certain volume of 10M methanol solution was added to one side. The same volume of deionized water was added to the other side. Magnetic stirrers were used on each compartment to ensure uniformity. Methanol concentration within the water cell was monitored by gas chromatography. The methanol diffusion coefficients were calculated by Fick's first law,[28] i.e.

$$C_{B(t)} = A\ V_B^{-1} DK\ L^{-1} C_A (t - t_0)$$

where C_A and C_B are the methanol concentrations of feed side and B side, respectively; A, L, and V_B are the effective area, the thickness of membrane, and the volume of permeated compartment, respectively; DK defined is the methanol permeability; t is time.

RESULTS AND DISCUSSION

Structure and Morphology of NFM and Composite Membranes

SBP is a new NF spinning method with high productivity. SPES and PES could form fibers easily using this method. Figure 1 shows SEM micrographs of solution blown SPES/PES NF and the corresponding diameter distribution map. SPES/PES NF had diameters between 100 and 900 nm. As shown in Figure 1(a), solution blown NF commonly curled in three dimensions and closely entangled. This structure was helpful not only to the mechanical properties, but also to the proton conduction because of the proton-conducting channels formed by NF.[8]

After impregnated into Nafion solution, Nafion flowed into the void space and then created a fully dense membrane structure after drying in air. Figure 2(a,b) present the 2D and 3D AFM micrographs of the surface morphology of NF/Nafion-20, respectively. SA (roughness average) value was only 1.96 nm, which indicated a compact and smooth membrane surface. The pores among NFs were completely filled with Nafion. Figure 2(c–e) show SEM images of the cross section of NF/Nafion-20, NF/Nafion-30, and NF/Nafion-40, respectively. It exhibits that NCMs had a reinforcing fiber mat of SPES/PES embedded in a Nafion matrix. No significant crack was observed, which indicated good compatibility between NFs and the Nafion phase.

The XRD curves of Nafion and NCMs are shown in Figure 3. For comparison, the curves of NCMs with different ratio, as well as pure Nafion and SPES/PES cast membrane, are given in the same figure. The peaks for SPES/PES and Nafion were broad and occurred at 2θ of 18° and 17°, respectively. For the composite membranes of NF/Nafion, two amorphous diffraction halos at $2\theta = 17°$ and 39° can be observed. This result was caused by the SPES/PES NF redistribution in Nafion and revealed the good compatibility of the materials.

Thermal Behavior

To evaluate the thermal stability of obtained membranes, TGA with the corresponding weight losses was recorded at a heating rate of 10°C per min under nitrogen gas to investigate the behavior of membranes with varied temperature, as shown in Figure 4. The curves exhibited three main degradation stages for all samples. The first step weight loss occurred between 80°C and 100°C, which was attributed to the loss of absorbed water molecules in the membrane matrix. The mass loss above 300°C corresponded to the loss of sulfonic acid groups. With increasing contents of NFs, NCMs presented a low mass loss, because they have less sulfonic acid groups than the other membranes. The third step weight loss of the composite membranes occurred at approximately 450°C, which represented the main chain degradation of polymers. These curves exhibited that Nation membrane possessed the most inferior thermal stability. All NF/Nafion membranes showed higher thermal stability than Nafion membrane. The thermal stability of NF/Nafion became

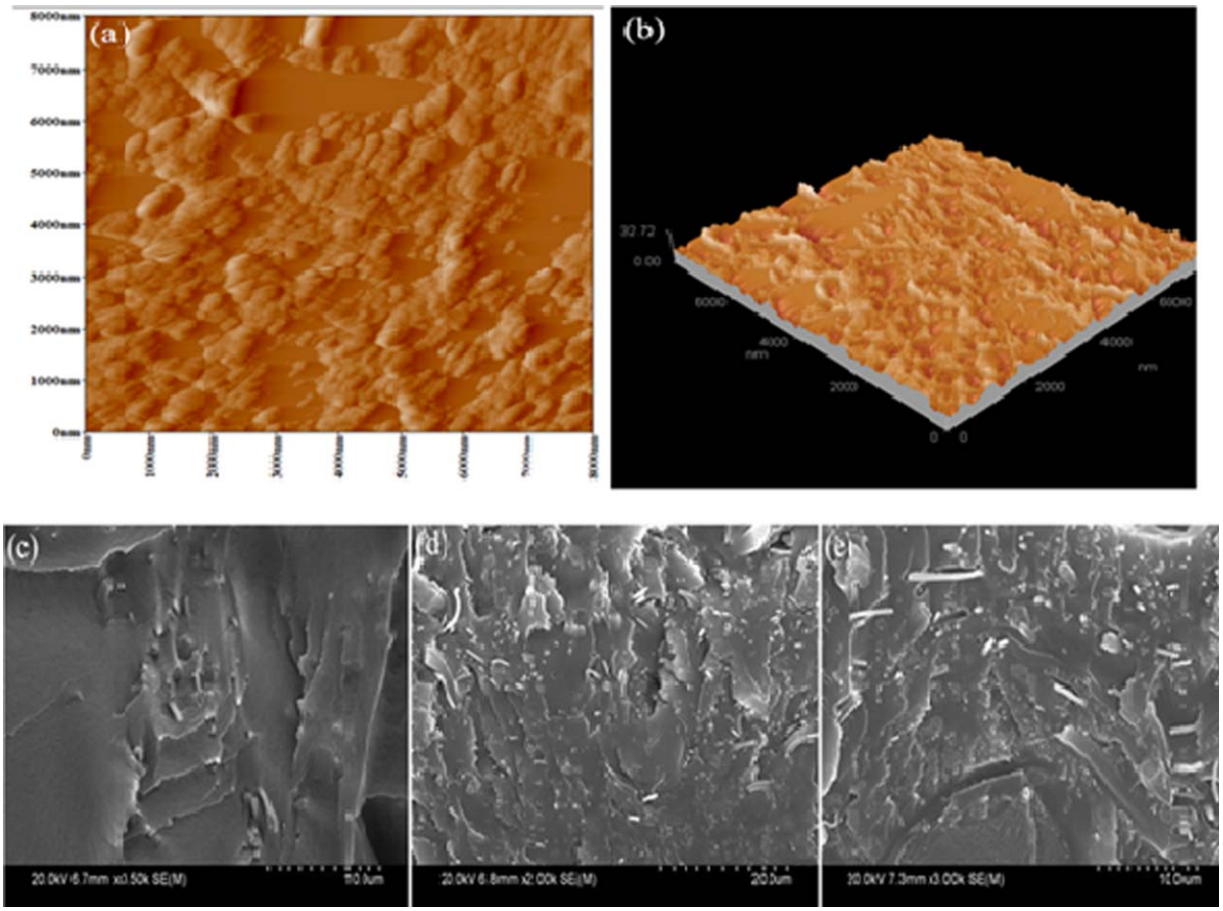

Figure 2. Micrographs of composite membrane, (a and b) 2D and 3D AFM images of NF/Nafion-20 surface, (c, d and e) SEM images of the cross-section of NF/Nafion-20, NF/Nafion-30, NF/Nafion-40. [Color figure can be viewed in the online issue, which is available at wileyonlinelibrary.com.]

better with the increasing contents of NF in membranes. SPES/PES NFM was the key to improve the thermal stability of the composite membranes. TGA experiments demonstrated that the composite membranes had a sufficient thermal stability to be used for fuel cell applications.

Proton Conductivity

Proton conduction capability is the most important characteristics of PEM for methanol fuel cell applications.[19] To evaluate the proton conductivity behavior of composite membranes, their proton conductivity was measured at different temperatures (20–80°C).

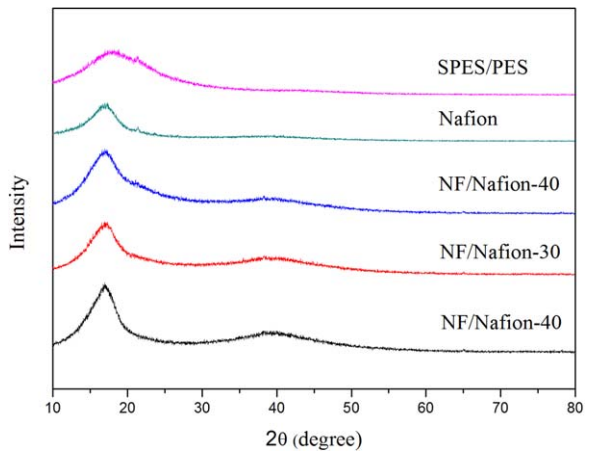

Figure 3. XRD patterns of SPES/PES, Nafion117, and NCMs. [Color figure can be viewed in the online issue, which is available at wileyonlinelibrary.com.]

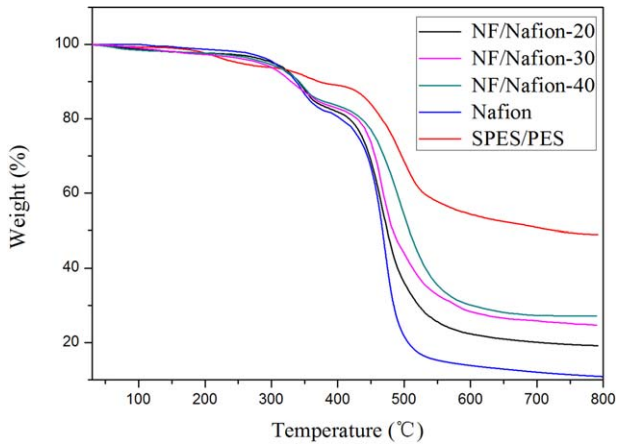

Figure 4. TGA of Nafion117, SPES/PES casting membranes and NCMs. [Color figure can be viewed in the online issue, which is available at wileyonlinelibrary.com.]

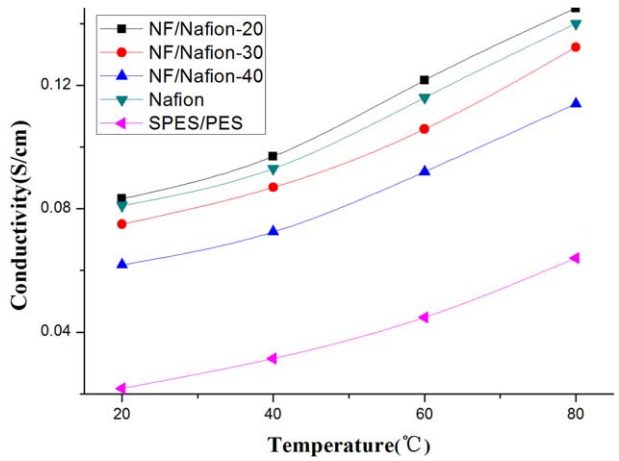

Figure 5. Proton conductivity–temperature relationship of Nafion117, SPES/PES casting membrane and NCMs. [Color figure can be viewed in the online issue, which is available at wileyonlinelibrary.com.]

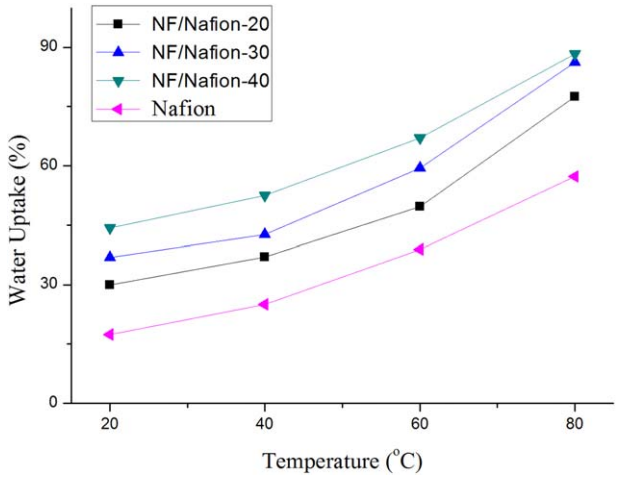

Figure 6. WU of Nafion117, SPES/PES casting membrane and NCMs. [Color figure can be viewed in the online issue, which is available at wileyonlinelibrary.com.]

Proton conductivity measurements were measured via four-point probe conductivity cell. Figure 5 represents the proton conductivity–temperature relationship of Nafion117, SPES/PES casting membrane and composite membranes. The proton conductivity of all the samples was improved by increasing temperature, which indicated that proton conduction was a thermally activated process. All NCMs showed higher proton conductivity than the casting membrane (SPES/PES). The proton conductivity of NF/Nafion- 20 composite membrane was higher than that of Nafion117 membrane. By contrast, the proton conductivity of the other two NCMs was lower than that of Nafion117 membrane. This result was ascribed to the fact that the existence of NF played a positive role for the proton conduction. NFs in composite membrane formed proton-conducting channels, through which the protons were transported rapidly and efficiently. The decreased proton conductivity with increasing contents of NF in membranes could be caused by the excess addition of NF with lower proton conductivity than Nafion. To conclude, the highest proton conductivity of NF/Nafion-20 was modestly superior to that of Nafion117 membranes in the temperatures range with a highest 4.8% increase than Nafion, and the highest conductivity got 0.145 S/cm. Therefore, the SPES/PES NCMs were suitable materials for DMFC.

Water Uptake and Swelling Ratio

Considering that PEM materials are mostly used in aqueous environments, WU and water stability are important characteristics of PEMs. The existence of water can enhance the proton conductivity of the membrane. However, high WU causes membrane swelling and reduce the use time. WU of different membranes is shown in Figure 6.

WU was correlated with the presence of SPES/PES NFs in the membrane. WU of NF/Nafion membranes was higher than that of Nafion at the same temperature. Hence, NF components contributed to attracting substantial water inside NF/Nafion membranes in comparison with pristine films. SPES also contains many polar groups along the backbone chain, which contribute to WU. The enhanced WU leads to higher proton conductivity for all the NCMs.

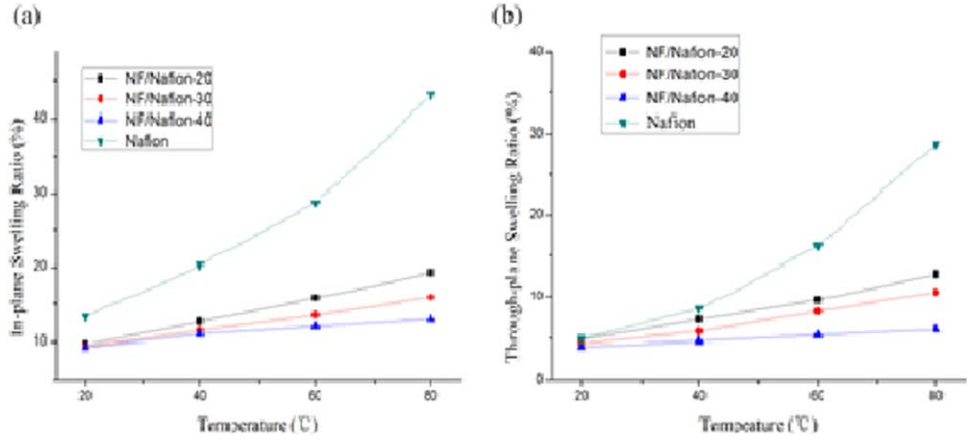

Figure 7. (a) IS of NF/Nafion-20, NF/Nafion-30, NF/Nafion-40, and Nafion117, (b) TS of NF/Nafion-20, NF/Nafion-30, NF/Nafion-40, and Nafion117. [Color figure can be viewed in the online issue, which is available at wileyonlinelibrary.com.]

Table I. Methanol Permeability, and Selectivity of Nafion, SPES/PES Casting Membrane and NCMs

Sample	Methanol permeability×10^{-7} (cm^2 s^{-1})	Selectivity (10^4 $sscm^{-3}$)
Nafion117	14.1	5.7
NF/Nafion-20	8.6	9.6
NF/Nafion-30	8.2	9.1
NF/Nafion-40	7.9	7.8
SPES/PES	3.4	6.4

The temperature dependence of IS and TS is shown in Figure 7. The Swelling Ratio (SR) values of NCMs were lower than those of Nafion117 and decreased with the increase of NF in impregnated membranes. On the contrary, both the SR values of impregnated membranes increased slowly with temperature in comparison with Nafion117. This phenomenon was the reinforcing effect, combined with the good compatibility between NF and the Nafion phase. Thus, the NCMs had improved dimensional stability by incorporation of SPES/PES NF into the Nafion matrix. The decrease in the IS was more pronounced than that in the TS. For instance, the IS and TS of Nafion117 was 43.08% and 28.75% at 80°C, respectively; the IS and TS of NF/Nafion-40 was 12.88% and 5.96%, which decreased by 30.2% and 24.45%, respectively. The transverse stretching of the NF was more difficult than the longitudinal stretching of the NF because of the more NF distribution in plane in the former.[13] Hence, NF skeleton limited the in-plane swelling more sufficiently than the through-plane swelling of the membranes.

Methanol Permeability

To prevent fuel from penetrating, PEMs used in DMFCs should possess a high methanol resistance property. Nevertheless, methanol crossover is a common problem to DMFC, especially to Nafion.

The methanol permeability of all samples was measured at room temperature, as shown in Table I. The results indicated that all novel membranes possessed more excellent methanol resistance property than Nafion117 did. The nanofibrous membranes showed remarkably reduced methanol permeability because of NF network structure, which may form a tortuous and anfractuous barrier layer to prevent methanol crossover.

Selectivity, which is the ratio of proton conductivity to methanol permeability, is usually a crucial factor for polymer electrolyte membrane to be used in DMFC.[29] Room-temperature selectivity values of all samples are also shown in Table I. Among all membranes, NF/Nafion-20 exhibited the highest selectivity, whereas Nafion117 showed the lowest selectivity. The improvement in selectivity could result from the incorporation of NF into Nafion.

CONCLUSION

PES was sulfonated with concentrated sulfuric acid. SPES/PES was fabricated to NFMs through solution blowing. Nafion-impregnated membranes were prepared successfully. The incorporation of SPS/PES NF into Nafion matrix improved the performance of NCMs as PEMs. The SPES/PES NF contributed to the formation of proton-conducting pathways and cut down the methanol permeability of the membrane as a barrier layer in the composite membrane. The proton conductivity of the NCMs was competitive with Nafion117. The proton conductivity of 20 wt % was better than that of Nafion117. Methanol permeability results showed that the incorporated SPES/PES NF acted as a methanol barrier layer to reduce methanol permeability. SR values showed that the presence of SPES/PES NF significantly improved dimensional stability. Overall, NF/Nafion-20 showed the best proton conductivity and NF/Nafion-40 showed the best dimensional stability and methanol permeability. These results suggested that such modified Nafion membranes could be potentially used in DMFCs.

ACKNOWLEDGMENTS

The author would like to thank Tianjin Natural Science Foundation (13JCZDJC32600) and Technology program of Tianjin Municipal Education Commission (20130324) for their financial support.

REFERENCES

1. Hasani-Sadrabadi, M. M.; Dashtimoghadam, E.; Majedi, F.; Kabiri, K.; Mokarram, N.; Solati-Hashjin, M.; Moaddel, H. *Chem. Commun.* **2010**, *46*, 6500.
2. Sharma, S.; Pollet, B. G. *J. Power Sources* **2012**, *208*, 96.
3. Hickner, M. A.; Ghassemi, H.; Kim, Y. S.; Einsla, B. R.; McGrath, J. E. *Chem. Rev.* **2004**, *104*, 4587.
4. Chang, B.-J.; Kim, D. J.; Kim, J. H.; Lee, S.-B.; Joo, H. J. *J. Membr. Sci.* **2008**, *325*, 989.
5. Li, Z.; He, G.; Zhao, Y.; Cao, Y.; Wu, H.; Li, Y.; Jiang, Z. *J. Power Sources* **2014**, *262*, 372.
6. Subramanian, M. S.; Sasikumar, G. *J. Appl. Polym. Sci.* **2010**, *117*, 801.
7. Changkhamchom, S.; Sirivat, A. *Solid State Ionics* **2014**, *263*, 161.
8. Li, H. and Y. Liu, *J. Mater. Chem. A* **2014**, *2*, 3783.
9. Zhuang, X.; Jia, K.; Cheng, B.; Feng, X.; Shi, S.; Zhang, B. *Chem. Eng. J.* **2014**, *237*, 308.
10. Yan, G.; Zhuang, X.; Tao, X.; Cheng, B. *Sci. Adv. Mater.* **2013**, *5*, 209.
11. Shi, L.; Zhuang, X.-p.; Cheng, B.-w.; Tao, X.-x.; Kang, W.-m. *Chn. J. Polym. Sci.* **2014**, *32*, 786.
12. Shi, S.; Zhuang, X.; Cheng, B.; Wang, X. *J. Mater. Chem. A* **2013**, *1*, 13779.
13. Shi, L.; Zhuang, X.; Tao, X.; Cheng, B.; Kang, W. *Fibers Polym.* **2013**, *14*, 1485.
14. Zhuang, X.; Cheng, B.; PhD; Guan, K.; Kang, W.; Ren, Y. *J. Eng. Fibers Fabrics* **2013**, *8*, 88.
15. Liu, R.; Xu, X.; Zhuang, X.; Cheng, B. *Carbohydr. Polym.* **2014**, *101*, 1116.

16. Xu, X.; Li, L.; Wang, H.; Li, X.; Zhuang, X.*RSC Adv.* **2014**, *5*, 4934.

17. Yin, Y.; Wang, J.; Yang, X.; Du, Q.; Fang, J.; Jiao, K. *Int. J. Hydrogen Energ* **2014**, *39*, 13671.

18. Pinar, F. J.; Cañizares, P.; Rodrigo, M. A; Úbeda, D.; Lobato, J. *J. Power Sources* **2015**, *274*, 177.

19. Shabani, I.; Hasani-Sadrabadi, M. M.; Haddadi-Asl, V.; Soleimani, M. *J. Membr. Sci.* **2011**, *368*, p. 233.

20. Hasani-Sadrabadi, M. M.; Shabani, I.; Soleimani, M.; Moaddel, H. *J. Power Sources* **2011**, *196*, 4599.

21. Takemori, R.; Kawakami, H. *J. Power Sources* **2010**, *195*, 5957.

22. Chae, K.-J.; Kim, K.-Y.; Choi, M.-J.; Yang, E.; Kim, I. S; Ren, X.; Lee, M. *Chem. Eng. J.* **2014**, *393*.

23. Wang, C.; Young Lee, S.; Won Shin, D.; Rae Kang, N.; Lee, Y. M. *J. Membr. Sci.* **2013**, *427*, 443.

24. Ballengee, J. B.; Pintauro, P. N. *J. Membr. Sci.* **2013**, *442*, 187.

25. Lee, J.-R.; Kim, N.-Y.; Lee, M.-S.; Lee, S.-Y.; Guiver, M. D. *J. Membr. Sci.* **2011**, *367*, 265.

26. Chul Gil, S.; Chul Kim, J.; Ahn, D.; Jang, J.-S.; Kim, .; Chul Jung, J.; Lim, S.; Jung, D.-H.; Lee, W. *J. Membr. Sci.* **2012**, *417–418*, 2.

27. Zhuang, X.; Yang, X.; Shi, L.; Cheng, B.; Guan, K.; Kang, W. *Carbohydr. Polym.* **2012**, *90*, 982.

28. Zhang, J.; Zhou, Z. *J. Power Sources* **2007**, *31*, 721.

29. Li, H.; Zhang, G.; Wu, J.; Zhao, C.; Zhang, Y.; Shao, K.; Han, M.; Lin, H.; Zhu, J.; Na, H. *J. Power Sources* **2010**, *195*, 6443.